

Analysis and design of profiled multiaperture stripline-to-microstrip couplers

K. Rambabu and J. Bornemann

Abstract: A new design methodology for a stripline-to-microstrip coupler is presented. Using circular apertures in their common ground plane, it is demonstrated that a design based on profiled circular apertures can be realised within a fraction of a wavelength while maintaining a comparable broadband behaviour. Various key points of the design, such as aperture dimensions and the number of apertures, are discussed. The analysis is based on weak coupling, and includes the mutual interactions of apertures. The theory is validated by measurements of prototypes with a constant, a sine and a cosine profile of apertures.

1 Introduction

One of the important aspects of component design is the trade-off between miniaturisation and power handling capability. Although miniaturisation has been generally achieved by utilising microstrip technology, the main application-oriented difference between microstrip and stripline circuits is their power handling capability [1]. If the performance of a stripline circuit at moderate power level is to be monitored through signal extraction by a weak coupler, it is often appropriate to design the control circuit in low-power microstrip technology in order to take advantage of its easier manufacturing and integration process. In many applications, a standard proximity coupler would be appropriate for such a task. In UHF and VHF bands, however, such an approach results in a relatively large component because of the required quarter-wavelength coupling section. To eliminate this restriction, a concept built on aperture coupling through a common ground plane has been presented in [2, 3]. One of the important specifications of the coupler is its directivity, which, in aperture couplers, depends on the shape of the aperture. Various shapes have been investigated by one of the authors in [4], with the result that, in order for a single aperture to achieve strong backward coupling and minimise forward coupling, circular apertures are recommended; therefore, they are employed here.

A large variety of coupler designs are available in the open literature. The majority, however, deal with symmetric configurations where the circuitry of main and coupled ports is identical. Such couplers are realised in either pure microstrip or pure stripline technology. This paper investigates, both theoretically and experimentally, the asymmetric stripline-to-microstrip coupler. To further reduce component size, different sets of profiled circular aperture arrangements are studied. The analysis includes mutual interactions of apertures, aperture averaging and well-known polarisability expressions. It will be demonstrated

that this design results in aperture arrangements of shorter overall component size while maintaining a relatively broadband performance.

2 Analysis

As shown in Figs. 1a and 1b, coupling is achieved through circular apertures in the common ground plane between the stripline and the microstrip configuration.

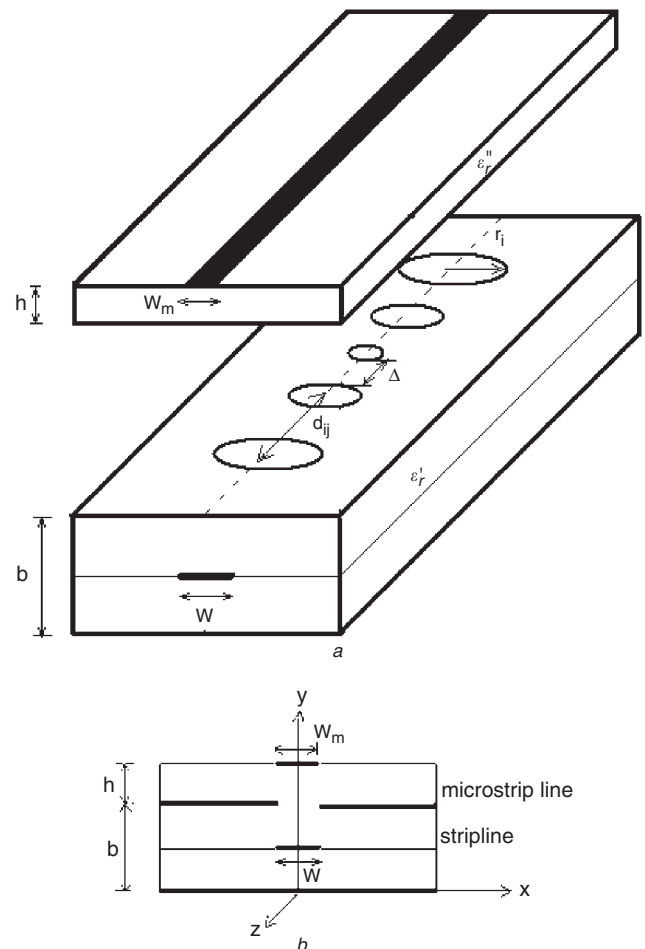


Fig. 1 Aperture-coupled strip-to-microstrip coupler
a 3-D view
b Cross-section

© IEE, 2003

IEE Proceedings online no. 20031086

doi:10.1049/ip-map:20031086

Paper first received 11th October 2002 and in revised form 17th September 2003

The authors are with the Department of Electrical and Computer Engineering, University of Victoria, P.O. Box 3055 Stn CSC, Victoria BC V8W 3P6, Canada

2.1 Single Aperture

Bethe's small aperture coupling theory, e.g. [5, 6], is used to characterise a single circular aperture. If the normal electric and tangential magnetic fields are not uniform over the coupling aperture, field averaging is required for the calculation of polarisation currents \mathbf{P}_e and \mathbf{P}_m . They are assumed at the centre of the aperture and are related to electric and magnetic current sources \mathbf{J} and \mathbf{M} , respectively, through

$$\mathbf{J} = j\omega\mathbf{P}_e = j\omega\epsilon_0\alpha_e \frac{\int \int E_n ds}{\int \int ds} \mathbf{n} \quad (1a)$$

$$\mathbf{M} = j\omega\mathbf{P}_m = -j\omega\alpha_m \frac{\int \int \mathbf{H}_t ds}{\int \int ds} \quad (1b)$$

where α_e and α_m are electric and magnetic polarisabilities, respectively.

Assuming the quasistatic mode of propagation for the microstrip line, the coupled fields can be represented by forward and backward traveling waves, which are expressed in terms of modal vectors \mathbf{e} and \mathbf{h} .

$$\begin{bmatrix} \mathbf{E}^+ \\ \mathbf{H}^+ \end{bmatrix} (z > 0) = C_{ec,mc}^+ \begin{bmatrix} \mathbf{e}_y \\ \mathbf{h}_x \end{bmatrix} e^{-j\beta_{gm}z} \quad (2a)$$

$$\begin{bmatrix} \mathbf{E}^- \\ \mathbf{H}^- \end{bmatrix} (z < 0) = C_{ec,mc}^- \begin{bmatrix} \mathbf{e}_y \\ -\mathbf{h}_x \end{bmatrix} e^{j\beta_{gm}z} \quad (2b)$$

Here, $C_{ec,mc}^\pm$ are the coupling coefficients owing to the corresponding sources in their respective directions, and β_{gm} is the propagation constant in the microstrip line. The coupling coefficients C can be determined by using the reciprocity theorem and the orthogonal property of the modal vectors:

$$C_{ec}^\pm = -\frac{1}{P_{ms}} \int_v \mathbf{e}_y \cdot \mathbf{J} dv \quad (3a)$$

$$C_{mc}^\pm = \mp \frac{1}{P_{ms}} \int_v \mathbf{h}_x \cdot \mathbf{M} dv \quad (3b)$$

where $P_{ms} = 2 \int_{s_0} (\mathbf{e}_y \times \mathbf{h}_x) \cdot z ds$, and s_0 is the cross-section of the microstrip line. The normalised TEM fields at the ground plane of the stripline can be represented by [7, 8]

$$E_y = \frac{-V}{b\sqrt{F(m)}} \left(\frac{1}{1 + m \sinh^2(\frac{\pi x}{b})} \right) e^{-j\beta_{gs}z} \quad (4a)$$

where

$$m = \operatorname{sech}\left(\frac{\pi W}{2b}\right) \quad (4b)$$

$$F(m) = \frac{8}{\left(\frac{b}{2}\right)^2} \int_{-\frac{b}{2}}^{\frac{b}{2}} \int_{-\infty}^{\infty} \frac{dx dy}{\left| 1 - m^2 \cosh^2 \frac{\pi(x + jy)}{b} \right|} \quad (4c)$$

b is the spacing between ground planes and W is the width of the stripline. Note that, contrary to simpler formulations available in the open literature (e.g. [6]), expressions (4) hold for symmetric as well as asymmetric configurations. By using a parallel-plate equivalent model for the microstrip line, the average power flow in the modal fields can be

written as

$$P_{ms} = \frac{2h^2}{Z_c} \quad (5)$$

where h is the thickness of the dielectric substrate and Z_c the characteristic impedance of the microstrip line.

The total coupling in the microstrip line in positive or negative z direction is the sum of the couplings resulting from the electric and magnetic currents. Therefore, couplings C^\pm in $\pm z$ directions are

$$C^+ = (C_{ec}^+ + C_{mc}^+) e_y e^{-j\beta_{gm}z}, \quad z > 0 \quad (6a)$$

$$C^- = (C_{ec}^- + C_{mc}^-) e_y e^{j\beta_{gm}z}, \quad z < 0 \quad (6b)$$

Following the reciprocity theorem and fundamental steps outlined in [2], the coupling coefficients in the forward and reverse direction can be written as

$$C^F = pF, \quad C^R = pR \quad (7a)$$

where

$$\begin{bmatrix} F \\ R \end{bmatrix} = \alpha_e \frac{\epsilon'_r \epsilon''_{reff}}{\epsilon'_r + \epsilon''_{reff}} \pm \alpha_m \sqrt{\epsilon'_r \epsilon''_{reff}} \quad (7b)$$

$$p = \frac{Z_c A}{120\lambda h^2 b \sqrt{F(m)}} \quad (7c)$$

A is a field averaging factor given by

$$A = \frac{\int \int \frac{1}{1 + m \sinh^2(\frac{\pi x}{b})} ds}{\int \int ds} \quad (7d)$$

and ϵ'_r , ϵ''_r are the dielectric constants of stripline and microstrip line, respectively; as shown in Figs. 1a and 1b.

Since stripline-to-microstrip couplers exhibit generally weak coupling, increasing a single aperture dimension or, alternatively, increasing the frequency of operation, i.e. reducing the wavelength, will not extend coupling beyond a certain level, thus saturating the amount of coupling. This is experimentally verified in Fig. 2 for a constant aperture size and varying frequency.

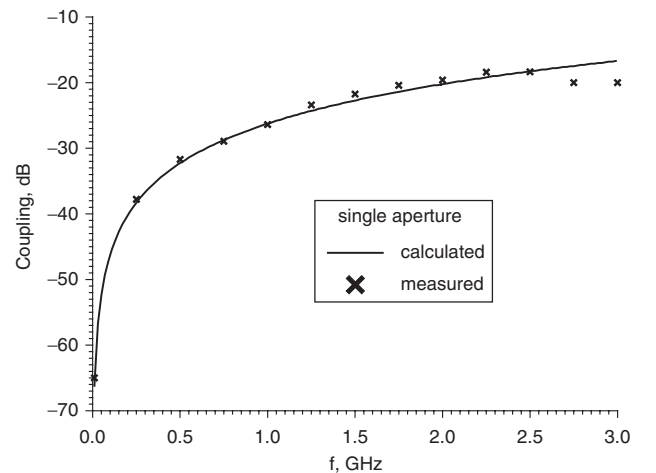


Fig. 2 Calculated and measured backward coupling of a single circular aperture

Radius = 4.1 mm, coupling in the common ground plane between stripline and microstrip line according to Fig. 1

This property sets the limit for the maximum aperture dimension. Coupling values and bandwidth are improved by utilising multiple apertures in some sort of tapered-size arrangement.

2.2 Multiple Apertures

In a multiaperture environment, the coupling value of a specific aperture is modified by the presence of fields of other apertures. Let the coupler have N apertures, and let the coupled field resulting from the i th aperture in the presence of other apertures in forward and reverse direction be $E_i^c F_i$ and $E_i^c R_i$, respectively. If the first (N th) aperture is considered, coupling is affected only by the reverse (forward) coupled fields of other apertures. The coupling at the i th aperture is affected by the forward coupled fields of $i-1$ apertures and the reverse coupled fields of the next $N-i$ apertures. Therefore, the effective coupling at the i th aperture can be written as

$$E_i^c = [p_i E_i^s - (E_1^c F_1 e^{-j\psi_{1i}} + \dots + E_{i-1}^c F_{i-1} e^{-j\psi_{(i-1)i}} + E_{i+1}^c R_{i+1} e^{-j\psi_{i(i+1)}} + \dots + E_N^c R_N e^{-j\psi_{iN}})] \quad (8)$$

where p , F , R are defined in (7), $\psi_{ij} = \beta_{gm} l_{ij}$, l_{ij} are the distances between the i th and j th apertures, and E_i^s is the field at the i th aperture in the stripline. These simultaneous equations form a matrix equation, which can be solved for effective coupling of an aperture in the presence of other apertures.

Finally, the total coupling of the multi-aperture coupler in forward direction is

$$E_T^F = 20 \log \left(\left| \sum_{i=1}^N E_i^c F_i e^{-j\psi_{iN}} \right| \right) \quad (9a)$$

and in reverse direction

$$E_T^R = 20 \log \left(\left| \sum_{i=1}^N E_i^c R_i e^{-j\psi_{iN}} \right| \right) \quad (9b)$$

With these equations, the performance of a profiled multiaperture strip-to-microstrip line coupler can be analysed and, for given line parameters, the lengths and aperture diameters synthesised.

It should be noted that (8) and (9) are based on the theory of small reflections, e.g. [9], and fail to include multiple reflections between successive apertures. However, it has been widely accepted that components operating on weak coupling can indeed be designed using this theory, e.g. [10], even though the assumption of small reflections might be violated [9].

3 Design

For design simplicity, we assume that the field over the aperture is uniform. It was found that the maximum aperture diameter, for which the assumption of a uniform field holds, is about eight percent of the guided wavelength. If the aperture dimension is too small, the coupling will vary drastically with frequency. Therefore, the ideal dimensions for the aperture are deemed to be between one and eight percent of the guided wavelength. Note that these limits may vary slightly with substrate thickness and dielectric constant.

Now consider a stripline with dielectric constant ϵ_r' and ground-to-ground spacing b , and a microstrip line with an effective dielectric constant ϵ_{reff}'' , e.g. [11], and thickness h , as shown in Figs. 1a and 1b. The characteristic impedance of the microstrip line is Z_c , the width of the stripline is w , and r is the radius of the aperture. For a single aperture coupler, the radius of the aperture for desired coupling C (dB) can be written as

$$r = (\varphi)^{1/3} \quad (10)$$

where

$$\varphi = \frac{180 \lambda h^2 b \sqrt{F(m)} 10^{-\frac{C(\text{dB})}{20}}}{Z_c \left[\frac{\epsilon_r' \epsilon_{reff}''}{\epsilon_r' + \epsilon_{reff}''} + 2 \sqrt{\epsilon_r' \epsilon_{reff}''} \right]} \quad (11)$$

and $F(m)$ and m are given in (4). Note that (11) follows from (7) by utilising standard expressions for polarisabilities α_e and α_m of circular apertures. If the calculated aperture radius in (10) exceeds the maximum value, more than one aperture is required to realise the desired coupling.

The first step of the design process is to specify substrate permittivities and thicknesses and the impedances of the strip and microstrip line. The second step is to select a constant minimum distance Δ as the gap between the edges of two successive apertures (cf. Fig. 1a). To minimise the size of the component, Δ should be kept as small as permissible by the manufacturing process.

If N apertures with radii r_i ($i = 1, \dots, N$) are used, then

$$\varphi = \left| \sum_{i=1}^N r_i^3 e^{-j(\beta_{gs} + \beta_{gms})d_{1i}} \right| \quad (12)$$

and the phase constants of the stripline and microstrip line are given by, respectively,

$$\beta_{gs} = \frac{2\pi}{\lambda} \sqrt{\epsilon_r'}, \quad \beta_{gms} = \frac{2\pi}{\lambda} \sqrt{\epsilon_{reff}''} \quad (13)$$

The spacings d_{1i} from the centre of the first aperture to the centre of the i -th aperture are:

$$d_{11} = 0, \quad d_{1i} = (r_1 + r_i) + 2 \sum_{k=2}^{i-1} r_k + (i-1)\Delta \quad (14)$$

They depend on the minimum distance Δ and the radii of the individual apertures. For uniform apertures ($r = r_1 = r_k = r_i$), (13) can be solved directly, thus yielding distances d_{1i} . For a coupler with profiled circular apertures, however, the radii of the apertures are not identical and can vary according to any functional form. Let δr be the minimum radius of the aperture, and let the radii follow a functional form f , e.g. sine or cosine, then the radii are given by

$$r_i = M \left[f \left(\frac{\pi(i-1)}{N-1} \right) + \delta r \right] \quad (15)$$

By substituting (15) in (12), the multiplication factor M can be deduced. The distances between aperture centres can then be calculated as described above.

3.1 Design Examples

Select the substrate parameters h , b , ϵ_r' and ϵ_{reff}'' , and calculate the width of the stripline and microstrip line for the required characteristic impedance. Compute the propagation constants β_{gs} and β_{gms} from (13). Next, specify the coupling 'C' to be achieved in dB. Calculate φ and then the radius from (11) and (10), respectively. If the calculated radius exceeds the maximum value, then multiple apertures are required for achieving the desired coupling.

3.1.1 Uniform aperture coupler

Let the number of apertures be six and have uniform radii ' r '. Let $\Delta = 2\text{mm}$ be the gap between edges of two successive apertures. Now, from (14), the distance between the apertures from the first aperture will be

$$d_{11} = 0, \quad d_{12} = 2r + \Delta \\ d_{13} = 4r + 2\Delta, \dots, d_{16} = 10r + 5\Delta \quad (16)$$

All the distances are functions of the radius r which can be calculated using (12).

3.1.2 Profiled aperture coupler

Let the design be the cosine-profiled coupler and have five apertures and δr be the minimum radius. From (15), the radii will be

$$\begin{aligned} r_1 = r_5 &= M[\cos(0) + \delta r], \\ r_2 = r_4 &= M\left[\cos\left(\frac{\pi}{4}\right) + \delta r\right], \\ r_3 &= M\left[\cos\left(\frac{\pi}{2}\right) + \delta r\right] \end{aligned} \quad (17)$$

The only unknown in (17) is M . Following (14), all distances d_{1i} can be represented in terms of r_1 to r_5 . Then M is calculated from (12).

The response of the coupler with frequency is (theoretically) periodic. The bandwidths of individual couplings are variable, and the first coupling band will have larger bandwidth compared to any other band. If the predicted diameter of an aperture is larger than the specified saturation limit, more apertures will be required to realise the desired coupling. The centre frequency of the coupling band can be tuned by adjusting the interaperture spacing. Coupling can be tuned by slightly modifying the aperture radius. The number of coupling bands within a broadband frequency range will increase with interaperture spacing within a band of frequencies.

4 Results

Using the above analysis and design guidelines, three stripline-to-microstrip couplers with varying profile of the apertures have been designed, built and measured. Unless specified differently, the circuits use $Z_c = 50 \Omega$, $\epsilon_r' = \epsilon_r'' = 2.32$, $b = 1.6$ mm, and $h = 0.8$ mm.

The first example is a 15-dB coupler with six identical apertures. By setting the minimum distance $\Delta = 2$ mm, the aperture radii are 4.1 mm from (12) and (14), and the centre-to-centre spacing is 10.2 mm. Figure 3 compares the calculated and measured coupling performance. Excellent agreement is observed, thus validating the analysis and design procedure.

The other two prototypes are shown in Fig. 4 which depicts, from left to right, the cosine profile of circular apertures, the (much longer) sine profile of apertures, the

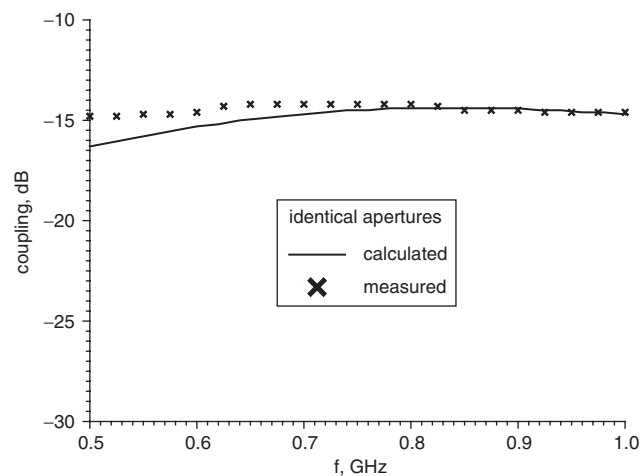


Fig. 3 Measured (xx) and calculated (solid line) coupling performance of stripline-to-microstrip coupler
Six identical apertures centered at 0.75 GHz

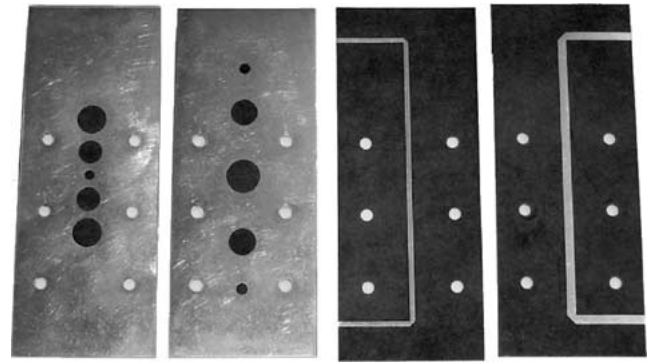


Fig. 4 Photograph of parts of the prototype aperture-coupled stripline-to-microstrip couplers
From left to right: aperture pattern of cosine profile, aperture pattern of sine profile, stripline circuit, and microstrip circuit

stripline, and the microstrip circuitry. The calculated and measured performance of the sine-profile coupler is shown in Fig. 5. The radii of the five apertures are 1.54, 3.72, 4.62, 3.72 and 1.54 mm. The distances between the centre of the first aperture and the centres of the following ones are 12.88, 31.08, 49.29 and 62.17 mm. The entire length of the coupler, measured from the left edge of the left-most aperture to the right edge of the right-most aperture, is only one third of the guided wavelength. Good agreement is observed between the measured and computed coupling (Fig. 5). The measured reflection coefficient is below -15 dB, and the maximum insertion loss is 2 dB in the upper frequency range, and below 1 dB for most of the band.

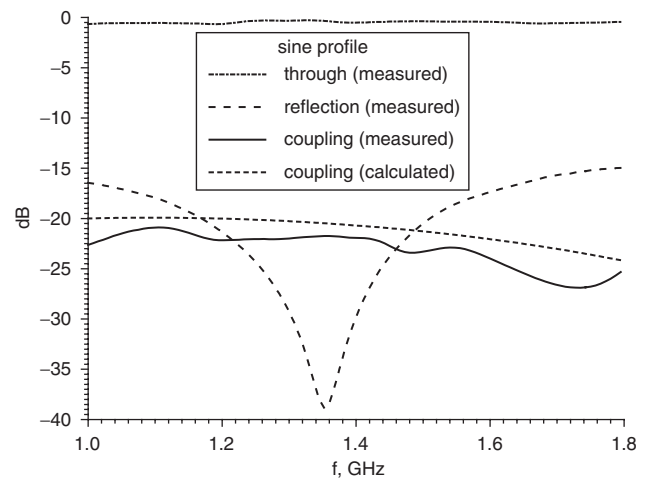


Fig. 5 Measured and computed results of strip-to-microstrip line coupler prototype with sine profile of circular apertures

Unfortunately, the prototype with the cosine profile was printed on a substrate with reduced thickness: 0.508 mm instead of 0.8 mm. This fact increases the coupling significantly. Moreover, the return loss is strongly influenced by the drastic change in characteristic impedance resulting from the reduced substrate heights. To be able to verify the design and analysis concept presented here, and demonstrate that the cosine profile yields smaller component size (one fifth of the guided wavelength; see Fig. 4) with comparable performance, the reduced substrate height was used in a recalculation of this coupler. Figure 6 shows a direct comparison of measured and calculated forward and

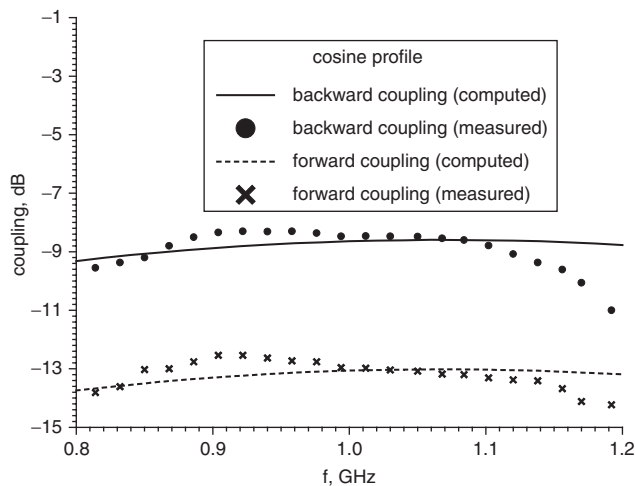


Fig. 6 Measured and computed coupling performance of strip-to-microstrip line coupler prototype with cosine profile of apertures

backward coupling for the cosine profile. Good agreement is observed for both coupling directions, thus verifying the theory presented in the previous Sections. (Note that a value of 9 dB can no longer be regarded as weak coupling. But the results confirm investigations in [10], according to which the weak coupling assumption holds up to approximately 10 dB.) However, Fig. 6 shows a decrease in coupling towards the end of the frequency band. This is a result of a return-loss variation from below 12 dB in the lower frequency range to 6 dB at 1.2 GHz, which follows directly from the mismatch caused by the thinner substrate. Of course, this influence was also visible in the transmission performance. Additionally an insertion loss in the 1 dB range with 0.45 dB variation was measured.

5 Conclusions

The simple analysis procedure offers an attractive solution for the design of aperture-coupled stripline-to-microstrip couplers. Although the theory is based on Bethe's small-aperture coupling theory, the design process is flexible and fairly accurate as it includes aperture averaging and mutual interactions in a multi-aperture environment. Simple guidelines provide the design engineer with reliable tools for the design of stripline-to-microstrip couplers. Three designs with different profiles of circular apertures are presented, and the validity of the design process is verified by experiments.

6 References

- 1 Wadell, B.C.: 'Transmission Line Design Handbook' (Artech House, 1991)
- 2 Jogiraju, G.V., and Pandharipande, V.M.: 'Stripline to microstrip line aperture coupler', *IEEE Trans. Microw. Theory Tech.*, 1990, **38**, pp. 440-443
- 3 Rambabu, K., and Kalghatgi, A.T.: 'Design equations for broadband planar aperture coupler', *IEEE Microw. Guid. Wave Lett.*, 1998, **8**, pp. 308-309
- 4 Rambabu, K., Keerti, K.S., Ramesh, M., and Kalghatgi, A.T.: 'Properties of various coupling apertures', *Microwave J.*, Aug. 2000, **43**, pp. 120-126
- 5 Bethe, H.A.: 'Theory of diffraction by small holes', *Phys. Rev.*, 1944, **66**, pp. 163-182
- 6 Collin, R.E.: 'Field theory of guided waves' (IEEE Press, 1991, 2nd edn.)
- 7 Rao, J.S., and Das, B.N.: 'Analysis of asymmetric stripline by conformal mapping', *IEEE Trans. Microw. Theory Tech.*, 1979, **27**, pp. 299-303
- 8 Rao, J.S., Joshi, K.K., and Das, B.N.: 'Analysis of inhomogeneously filled stripline and microstrip line', *IEE Proc. H, Microw., Optics Antennas*, 1980, **127**, pp. 11-14
- 9 Cohn, S.B.: 'Optimum design of stepped transmission-line transformers', *IRE Trans. Microw. Theory Tech.*, 1955, **3**, pp. 16-21
- 10 Sieverding, T., Papziner, U., and Arndt, F.: 'Mode-matching CAD of rectangular or circular multiaperture narrow-wall couplers', *IEEE Trans. Microw. Theory Tech.*, 1997, **45**, pp. 1034-1040
- 11 Hoffmann, R.K.: 'Handbook of microwave integrated circuits' (Artech House, 1987)